





Cite this: *Chem. Commun.*, 2018, 54, 3629

Received 8th February 2018,
Accepted 16th March 2018

DOI: 10.1039/c8cc01132j

rsc.li/chemcomm

The active role of Ca^{2+} ions in $\text{A}\beta$ -mediated membrane damage†

Michele F. M. Sciacca,^a Irene Monaco,^a Carmelo La Rosa ^{*b} and Danilo Milardi ^{*a}

Calcium dysregulation, membrane leakage and $\text{A}\beta$ amyloid growth are hallmarks of Alzheimer's disease. Here we show that Ca^{2+} ions inhibit membrane damage due to amyloid channels but enhance membrane disruption associated with fibers growing on the lipid surface. The similarities with IAPP suggest that this may represent a mechanism common to all proteinopathies.

Alzheimer's disease (AD) is the most common type of senile dementia, affecting an increasingly large population of elderly people in industrialized countries. A remarkable pathological hallmark of AD is the presence of extracellular proteinaceous deposits in the brain, termed senile plaques. The major component of senile plaques is the β -amyloid peptide ($\text{A}\beta$).¹ Although the molecular events underlying the development of AD remain elusive, there is a large consensus on the key role played by $\text{A}\beta$ aggregation in causing neuronal death.² $\text{A}\beta$ peptides have been reported to initiate several, intertwined pathological events on neurons including: (i) production of reactive oxygen species (ROS), (ii) endoplasmic reticulum (ER) stresses, and (iii) an increase in intracellular calcium levels ($[\text{Ca}^{2+}]_i$).³ One of the mechanisms accounting for $\text{A}\beta$ -induced toxicity is based on the formation of peptide channels by the direct insertion of $\text{A}\beta$ into membranes (amyloid channel hypothesis).^{4–6} However, there are significant discrepancies between experimental results reported by different authors for the biophysical properties of membrane-bound $\text{A}\beta$ peptides. Previous reports by some of us have evidenced that $\text{A}\beta$ induces membrane damage *via* a two-step mechanism which involves (i) the binding of peptide oligomers to the membrane to form ion permeable channels and (ii) fiber growth on the lipid surface causing lipid loss *via* a detergent-like mechanism.⁷ The interaction of $\text{A}\beta$ with different membrane lipids was examined

by several groups and the only lipids that were found to bind $\text{A}\beta$ were the negatively charged gangliosides^{8–10} and phosphatidylserine (PS)-rich membranes.^{11,12} Of note, the presence of negatively charged lipids is not sufficient for driving $\text{A}\beta$ -membrane binding and there is evidence that these lipids need to be clustered in order to foster interaction with $\text{A}\beta$.¹³ Therefore, besides lipid composition, several adverse environmental factors are expected to play a key role in driving abnormal membrane- $\text{A}\beta$ interactions. Ca^{2+} ions, in particular, induce lipid phase segregation by recruiting negatively charged lipids on the membrane surface^{14,15} and regulate many membrane-related activities including the formation of membrane domains,¹⁶ membrane fusion and vesicles trafficking.¹⁷ All these findings point to a close relationship between calcium dyshomeostasis, aberrant $\text{A}\beta$ membrane interaction and, eventually, toxicity. In two previous papers we have demonstrated that Ca^{2+} ions favor the interaction of islet amyloid polypeptide—an amyloidogenic peptide implicated in type 2 diabetes mellitus pathogenesis—with the hydrophobic core of PS membranes,¹⁸ thus causing lipid loss from PS model membranes *via* a detergent-like mechanism.¹⁹ Since both types of membrane-damage mechanisms (*i.e.* poration and detergent-like effects) are common to $\text{A}\beta$ and IAPP, it is therefore reasonable to think that calcium dyshomeostasis may be a part of a general mechanism underlying amyloid membrane damage.

To verify this hypothesis, here we investigate the effect of Ca^{2+} ions on the $\text{A}\beta$ -mediated membrane leakage by using an array of different physico-chemical techniques. To evaluate the effect of Ca^{2+} ions on the structure of $\text{A}\beta_{1-40}$, we first performed CD experiments (see Fig. S1 of the ESI†). We did not observe any significant secondary structure variation in the range of concentrations explored. Thus, monomeric $\text{A}\beta_{1-40}$ assumes a random coil conformation independently from the presence of Ca^{2+} ions. Next, to investigate the influence of Ca^{2+} ions on $\text{A}\beta_{1-40}$ fiber growth, we performed ThT experiments on $\text{A}\beta_{1-40}$ samples containing increasing amounts of Ca^{2+} ions. Samples containing a substoichiometric amount of Ca^{2+} (Fig. 1, red curve) did not affect the fiber growth. By contrast, on increasing the Ca^{2+} concentration (see Fig. 1, green curve), we observed a significant decrease of

^a Istituto di Biostrutture e Bioimmagini, Consiglio Nazionale delle Ricerche, Sede Secondaria di Catania, Via Paolo Gaifami 18, 95126, Catania, Italy. E-mail: danilo.milardi@cnr.it

^b Università degli Studi di Catania, Dipartimento di Scienze Chimiche, Viale Andrea Doria 6, 95125 Catania, Italy. E-mail: clarosa@unict.it

† Electronic supplementary information (ESI) available: Materials and methods, CD spectra and western blot experiments. See DOI: 10.1039/c8cc01132j

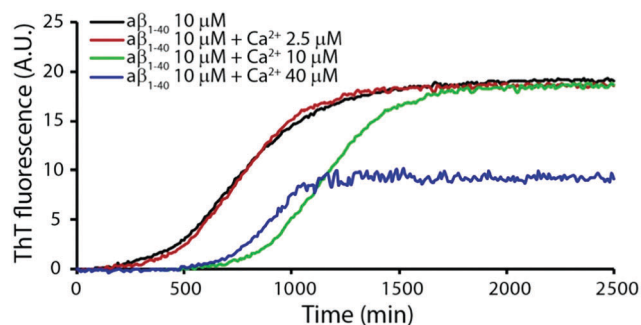


Fig. 1 Effect of Ca^{2+} on $\text{A}\beta_{1-40}$ fiber formation kinetics. ThT traces of samples containing $\text{A}\beta_{1-40}$ 10 μM (black) in the presence of Ca^{2+} 2.5 μM (red), Ca^{2+} 10 μM (green) and Ca^{2+} 40 μM (blue). Experiments were performed at 37 $^{\circ}\text{C}$ in 10 mM HEPES buffer, 100 mM NaCl, pH 7.4. All results are the average of three experiments. Further experimental details are reported in the ESI†

fiber growth kinetics although the total amount of fiber formed remained substantially the same as the control. Notably, excess Ca^{2+} ions decrease both the total mass of fiber formed and fiber formation kinetics. Ca^{2+} ions may thus influence the amyloid growth pathway (see Table 1).

To evaluate the effect of Ca^{2+} ions on small-sized oligomeric assemblies, we performed western blot analysis of Ca^{2+} enriched $\text{A}\beta$ samples at different incubation times (see Fig. S2 in the ESI†). The results show that Ca^{2+} ions inhibit the formation of oligomers in accordance with ThT assays, evidencing the inhibition of fiber growth.

Next, ThT experiments were also carried out in the presence of model membranes with a neuron-mimicking lipid composition. To this aim the effects of Ca^{2+} ions on fiber formation were investigated by using large unilamellar vesicles (LUVs) composed of total lipid brain extract (TLBE) (Fig. 2). In open contrast with the results obtained in aqueous solution, increasing the amounts of Ca^{2+} ions in the presence of LUV TLBE increases both the fiber formation kinetics and the total amount of fiber (Table 2).

This evidence is consistent with western blot results (see Fig. S3 in the ESI†) and supports the hypothesis that Ca^{2+} ions promote the formation of $\text{A}\beta$ oligomers and, in turn, foster fiber formation. We next tested the effects of Ca^{2+} ions on $\text{A}\beta$ -mediated membrane damage by using 6-carboxyfluorescein in dye release experiments (Fig. 3). We observe that at low Ca^{2+} concentration the mechanism of membrane disruption occurs *via* a two-step mechanism⁷ (Fig. 3, black and red curves): an initial immediate release of the dye, due

Table 1 Kinetic parameters of ThT traces relative to samples shown in Fig. 1, calculated as reported in the ESI. ThT_{max} is the maximum value of the ThT signal, which is correlated with the total mass of fiber formed; $t_{1/2}$ is the time the signal needs to reach 50% of the maximum; and k is the apparent growth rate of fiber. All parameters are reported as the average of 3 independent measurements \pm s.d.

Sample	ThT_{max} (a.u.)	$t_{1/2}$ (min)	$k \times 10^3$ (min^{-1})
$\text{A}\beta_{1-40}$ 10 μM	18.8 ± 3.1	776 ± 2	5.5 ± 0.016
$\text{A}\beta_{1-40}$ 10 μM + Ca^{2+} 2.5 μM	18.5 ± 1.8	769 ± 2	6.6 ± 0.043
$\text{A}\beta_{1-40}$ 10 μM + Ca^{2+} 10 μM	18.4 ± 2.2	1157 ± 3	6.7 ± 0.045
$\text{A}\beta_{1-40}$ 10 μM + Ca^{2+} 40 μM	9.3 ± 2.6	885 ± 3	6.9 ± 0.026

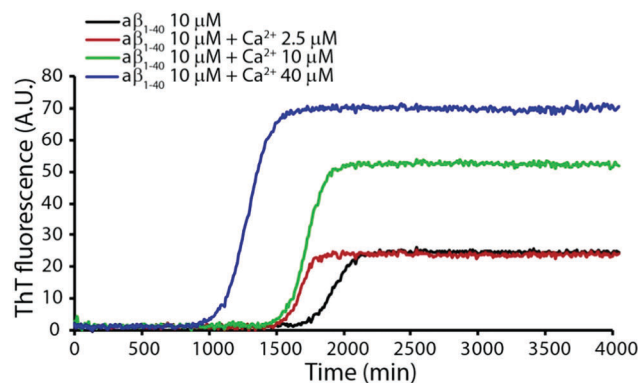


Fig. 2 Effect of Ca^{2+} on $\text{A}\beta_{1-40}$ fiber formation kinetics in the presence of LUV TLBE. ThT traces of samples containing 200 μM LUV TLBE and $\text{A}\beta_{1-40}$ 10 μM (black) in the presence of Ca^{2+} 2.5 μM (red), Ca^{2+} 10 μM (green) and Ca^{2+} 40 μM (blue). Experiments were performed at 37 $^{\circ}\text{C}$ in 10 mM HEPES buffer, 100 mM NaCl, pH 7.4. All results are the average of three experiments.

Table 2 Kinetic parameters of ThT traces relative to samples shown in Fig. 2. All parameters are reported as the average of 3 independent measurements \pm s.d.

Sample + LUV TLBE	ThT_{max} (a.u.)	$t_{1/2}$ (min)	$k \times 10^3$ (min^{-1})
$\text{A}\beta_{1-40}$ 10 μM	23.7 ± 1.5	1920 ± 6	1.3 ± 0.088
$\text{A}\beta_{1-40}$ 10 μM + Ca^{2+} 2.5 μM	21.4 ± 3.2	1683 ± 13	2.3 ± 0.054
$\text{A}\beta_{1-40}$ 10 μM + Ca^{2+} 10 μM	50.5 ± 2.1	1724 ± 4	1.5 ± 0.078
$\text{A}\beta_{1-40}$ 10 μM + Ca^{2+} 40 μM	69.8 ± 2.2	1279 ± 4	1.2 ± 0.042

to pore formation, and a second step correlated with the elongation of the fiber on the membrane surface resulting in a detergent-like membrane disruption mechanism. By contrast, on increasing the Ca^{2+} concentration, the first step vanishes (Fig. 3 blue and green curves), suggesting that Ca^{2+} ions inhibit pore formation. This result matches well with the hypothesis that calcium ions stabilize small-sized oligomeric species.

However, it is known that, due to their small size, pores formed by $\text{A}\beta_{1-40}$ are only barely detected *via* dye leakage experiments with 6-carboxyfluorescein.⁷ Thus, to analyze the effects of Ca^{2+} ions on the first step of the membrane damage

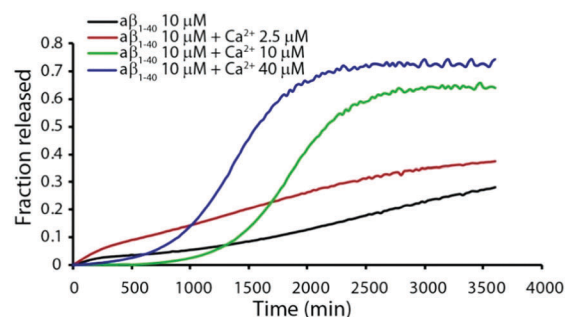


Fig. 3 Membrane disruption induced by $\text{A}\beta_{1-40}$ in the presence of Ca^{2+} . Disruption of 200 μM LUV TLBE induced by 10 μM $\text{A}\beta_{1-40}$ (black) in the presence of Ca^{2+} 2.5 μM (red), Ca^{2+} 10 μM (green curve) and Ca^{2+} 40 μM (blue). Experiments were performed at 37 $^{\circ}\text{C}$ in 10 mM HEPES buffer, 100 mM NaCl, pH 7.4. All results are the average of three experiments.

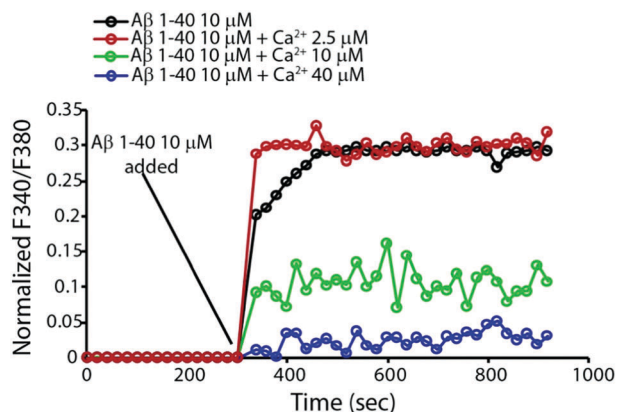


Fig. 4 The presence of Ca^{2+} inhibits the pore formation. Fura 2 assay indicates that increasing amounts of Ca^{2+} ions inhibit disruption through pore formation of 200 μM LUV TLBE induced by 10 μM $\text{A}\beta_{1-40}$ (black) in the presence of Ca^{2+} 2.5 μM (red), Ca^{2+} 10 μM (green) and Ca^{2+} 40 μM (blue). Experiments were performed in 10 mM HEPES buffer, 100 mM NaCl, pH 7.4.

mechanism, we performed dye-release experiments using the dye Fura 2 as described elsewhere⁷ (Fig. 4).

Data reported in Fig. 4 show that the presence of a high concentration of Ca^{2+} ions inhibits pore formation. Consistently with data previously reported for hIAPP,^{18,19} all of the results obtained here support the hypothesis that Ca^{2+} ions inhibit $\text{A}\beta$ -mediated membrane poration but enhance membrane fragmentation by lipid loss due to fiber growth on the membrane surface. In conclusion, it is plausible that this double-edged effect of Ca^{2+} ions on amyloid-evoked membrane disruption processes may represent a general feature shared by all proteinopathies. Due to the key role played by calcium dyshomeostasis in many amyloid diseases, further studies on other amyloidogenic proteins such as α -synuclein or huntingtin will be important to support the generality of this biophysical mechanism.

This work was financially supported by the Italian MiUR program PRIN 20157WZM8A.

Conflicts of interest

There are no conflicts to declare.

Notes and references

- 1 D. J. Selkoe, *Neuron*, 1991, **6**, 487–498.
- 2 J. Hardy and D. J. Selkoe, *Science*, 2002, **297**, 353–356.
- 3 D. H. Small, S. S. Mok and J. C. Bornstein, *Nat. Rev. Neurosci.*, 2001, **2**, 595–598.
- 4 N. Arispe, J. C. Diaz and O. Simakova, *Biochim. Biophys. Acta, Biomembr.*, 2007, **1768**, 1952–1965.
- 5 H. A. Lashuel and P. T. Lansbury, *Q. Rev. Biophys.*, 2006, **39**, 167–201.
- 6 M. Kawahara, M. Negishi-Kato and Y. Sadakane, *Expert Rev. Neurother.*, 2009, **9**, 681–693.
- 7 M. F. M. Sciacca, S. A. Kotler, J. R. Brender, J. Chen, D. Lee and A. Ramamoorthy, *Biophys. J.*, 2012, **103**, 702–710.
- 8 A. Kakio, S. I. Nishimoto, K. Yanagisawa, Y. Kozutsumi and K. Matsuzaki, *J. Biol. Chem.*, 2001, **276**, 24985–24990.
- 9 A. Kakio, S. Nishimoto, K. Yanagisawa, Y. Kozutsumi and K. Matsuzaki, *Biochemistry*, 2002, **41**, 7385–7390.
- 10 K. Ikeda and K. Matsuzaki, *Biochem. Biophys. Res. Commun.*, 2008, **370**, 525–529.
- 11 N. Arispe, E. Rojas and H. B. Pollard, *Proc. Natl. Acad. Sci. U. S. A.*, 1993, **90**, 567–571.
- 12 T.-L. Lau, E. E. Ambroggio, D. J. Tew, R. Cappai, C. L. Masters, G. D. Fidelio, K. J. Barnham and F. Separovic, *J. Mol. Biol.*, 2006, **356**, 759–770.
- 13 K. Matsuzaki, *Acc. Chem. Res.*, 2014, **47**, 2397–2404.
- 14 S. Ohnishi and T. Ito, *Biochemistry*, 1974, **13**, 881–887.
- 15 S. Tamamizu-Kato, M. G. Kosaraju, H. Kato, V. Raussens, J.-M. Ruyschaert and V. Narayanaswami, *Biochemistry*, 2006, **45**, 10947–10956.
- 16 V. Gerke, C. E. Creutz and S. E. Moss, *Nat. Rev. Mol. Cell Biol.*, 2005, **6**, 449–461.
- 17 U. Rescher and V. Gerke, *J. Cell Sci.*, 2004, **117**, 2631–2639.
- 18 M. F. M. Sciacca, M. Pappalardo, D. Milardi, D. M. Grasso and C. La Rosa, *Arch. Biochem. Biophys.*, 2008, **477**, 291–298.
- 19 M. F. M. Sciacca, D. Milardi, G. M. L. Messina, G. Marletta, J. R. Brender, A. Ramamoorthy and C. La Rosa, *Biophys. J.*, 2013, **104**, 173–184.